Eur. Phys. J. D (2017) 71: 23
DOI: 10.1140/epjd/e2016-70616-4

THE EUROPEAN PHYSICAL JOURNAL D

Regular Article

Electron momentum spectroscopy of H_2^+ in the presence of laser radiation*

Andrew A. Bulychev[1,a] and Konstantin A. Kouzakov[2]

[1] Laboratory of Theoretical Physics, Joint Institute for Nuclear Research, Moscow Region, Dubna 141980, Russia
[2] Department of Nuclear Physics and Quantum Theory of Collisions, Faculty of Physics, Lomonosov Moscow State University, Moscow 119991, Russia

Received 30 September 2016 / Received in final form 1 December 2016
Published online 7 February 2017 – © EDP Sciences, Società Italiana di Fisica, Springer-Verlag 2017

Abstract. Theoretical analysis of laser-assisted electron impact ionization of a hydrogen molecular ion H_2^+ at high impact energy and large momentum transfer is carried out. The laser-field effects on the incoming and outgoing electrons are taken into account using the Volkov functions. The field-dressing of the target electron is treated with a quasistatic state approach. Calculations for laser radiation with frequency $\omega = 1.55$ eV and intensity $I = 5 \times 10^{11}$ W/cm^2 exhibit strong laser influence on the molecular bond oscillation in laser-assisted electron momentum distributions.

1 Introduction

Electron impact ionization at high impact energy and large momentum transfer, often referred to as electron momentum spectroscopy (EMS), provides a unique opportunity for direct measurement of electron momentum distribution in atoms and molecules [1–3]. Recently, a new application of this method has emerged, which is called time-resolved EMS [4,5], where the laser system is combined with an EMS spectrometer. This novel technique measures electron momentum distributions in a pump-and-probe mode, with a laser pulse being a pump and a usual $(e, 2e)$ EMS being a probe. The developed apparatus also can be applied to conduct EMS measurements on atomic and molecular targets in the presence of laser radiation, which amounts to the laser-assisted EMS method [6]. This calls for theoretical investigations on the potential of laser-assisted EMS to study laser effects on electronic structure of atoms and molecules.

So far, the theoretical analysis of the laser-assisted EMS has been focused on the case of atomic targets, such as atomic hydrogen [6,7] and helium [8,9]. In particular, a general theoretical framework for laser-assisted EMS was formulated in [6], where it was applied to atomic hydrogen, which is a benchmark system for EMS. Later this approach was extended to the He atom, with special attention to manifestation of electron-electron correlation effects in ionization-excitation and double ionization processes [8,9]. It should be noted that from an experimental point of view the He atom is a more convenient target than atomic hydrogen. Another possible candidate for a laser-assisted EMS experiment is an H_2 molecule. However, in the case of molecular targets, a number of effects of laser field on the target can be expected, ranging from laser-induced molecular axis alignment to laser-induced molecular dissociation. For this reason, our present theoretical analysis is devoted to laser-assisted EMS of a molecular system. We limit ourselves to the case of the H_2^+ ion, focusing on the one-electron dynamics in a field-dressed molecule, and inspect laser-field influence on the momentum profiles. Specifically, we examine how the presence of a laser field can affect the bond oscillation effect, which has been experimentally observed with EMS technique for molecular targets [10–12].

The paper is organized as follows. Section 2 describes our theoretical framework for the laser-assisted EMS of H_2^+. In Section 3, numerical results are presented and discussed. The conclusions are formulated in Section 4.

2 Theory

We consider the case of the $(e, 2e)$ process taking place on the H_2^+ ion in the presence of laser radiation specified by

$$\boldsymbol{F}(t) = \boldsymbol{F}_0 \cos\omega t, \qquad \boldsymbol{A}(t) = -\frac{c}{\omega}\boldsymbol{F}_0 \sin\omega t,$$

where $\boldsymbol{F}$ and $\boldsymbol{A}$ are the electric field and vector potential, respectively. In order to discard possible photoionization and photodissociation effects, the laser electric-field amplitude $\boldsymbol{F}_0$ must be small compared to the typical intramolecular field. In what follows, the incident, scattered

* Contribution to the Topical Issue "Many Particle Spectroscopy of Atoms, Molecules, Clusters and Surfaces", edited by A.N. Grum-Grzhimailo, E.V. Gryzlova, Yu V. Popov, and A.V. Solov'yov.

[a] e-mail: bulychev@theor.jinr.ru

and ejected electron energies and momenta are specified by respectively $(E_0, \boldsymbol{p}_0)$, $(E_s, \boldsymbol{p}_s)$ and $(E_e, \boldsymbol{p}_e)$.

Using the first Born and binary-encounter approximations, the S-matrix for the laser-assisted EMS process is evaluated as [6]

$$S = -i \int_{-\infty}^{\infty} dt \langle \chi_{\boldsymbol{p}_s}(t) \chi_{\boldsymbol{p}_e}(t) \, |v_{ee}| \, \chi_{\boldsymbol{p}_0}(t) \Psi_i(t) \rangle, \qquad (1)$$

where $\chi_{\boldsymbol{p}}$ stands for the incoming and outgoing electron states, Ψ_i is the laser-dressed initial H_2^+ state, and v_{ee} is the Coulomb potential between the colliding electrons. The validity of the expression (1) is restricted to the kinematical regime of high impact energy and large momentum transfer. In addition, the value of the momentum

$$\boldsymbol{q} = \boldsymbol{p}_s + \boldsymbol{p}_e - \boldsymbol{p}_0$$

is supposed to be much smaller than p_0, p_s, and p_e and to lie in the range of momentum values typical for target electrons.

The incoming and outgoing electron states are described in terms of Volkov functions [13], which in the length gauge are given by [14]

$$\chi_{\boldsymbol{p}}(\boldsymbol{r}, t) = \exp\left\{ i \left[\boldsymbol{p} \cdot \boldsymbol{r} - \alpha_{\boldsymbol{p}} \cos \omega t - Et - \zeta(t) + \frac{1}{c} \boldsymbol{A}(t) \cdot \boldsymbol{r} \right] \right\}, \qquad (2)$$

where

$$E = \frac{p^2}{2}, \qquad \alpha_{\boldsymbol{p}} = \frac{\boldsymbol{p} \cdot \boldsymbol{F}_0}{\omega^2}, \qquad \zeta(t) = \frac{1}{2c^2} \int_{-\infty}^{t} A^2(t') dt'.$$

If one neglects the laser-field effects on the incoming and outgoing electrons, then the Volkov solution (2) reduces to a usual plane wave,

$$\chi_{\boldsymbol{p}}(\boldsymbol{r}, t) = \exp[i(\boldsymbol{p} \cdot \boldsymbol{r} - Et)]. \qquad (3)$$

In references [7,15], the plane-wave and Volkov-function treatments were compared and the latter was shown to be necessary to obtain accurate results for the laser-assisted momentum profiles.

We treat the H_2^+ molecular ion within the Born-Oppenheimer approach, separating nuclear and electron dynamics. The laser-field influence on the electron states of the ion is accounted for within a quasistatic-states framework [16–18]. Such an approach goes beyond the usual perturbation theory and it has proved to be efficient in describing dynamics of the H_2^+ ion in a laser field. In this method, a time-dependent Schrödinger equation $i\partial_t \phi = \hat{H}\phi$ is approximated by a stationary-like form $\hat{H}\phi = E(t)\phi$ with time-dependent energy eigenvalues. When the field-free ϕ_g and ϕ_u states, constructed from $1s$ atomic orbitals as

$$\phi_g = N_g \left[\phi_{1s}(\boldsymbol{r} + \boldsymbol{R}/2) + \phi_{1s}(\boldsymbol{r} - \boldsymbol{R}/2) \right], \qquad (4)$$

$$\phi_u = N_u \left[\phi_{1s}(\boldsymbol{r} + \boldsymbol{R}/2) - \phi_{1s}(\boldsymbol{r} - \boldsymbol{R}/2) \right], \qquad (5)$$

are used as a basis to expand the solutions of this equation, the resulting quasistatic states are given by

$$\phi_1 = \cos\theta \phi_g + \sin\theta \phi_u, \quad \phi_2 = -\sin\theta \phi_g + \cos\theta \phi_u, \quad (6)$$

$$\tan 2\theta = \frac{-2\langle \phi_g | \boldsymbol{r} \boldsymbol{F}(t) | \phi_u \rangle}{E_u(R) - E_g(R)}, \qquad (7)$$

where $\boldsymbol{R}$ is the internuclear axis vector and $E_g(R)$ and $E_u(R)$ are field-free molecular orbital energies. The initial H_2^+ state should also take into account a nuclear subsystem. We assume that the nuclear motion remains unaffected by the laser field and that the ion is in the ground rotational and vibrational states

$$\Psi_i = \psi_g(\boldsymbol{R}, t) \phi_1(\boldsymbol{r}, \boldsymbol{R}, t), \qquad (8)$$

where $\psi_g(\boldsymbol{R}, t)$ is a ground-state nuclear wave function corresponding to the ϕ_g electronic term.

The final continuum state of the nuclear subsystem after the ionization is not resolved. Neglecting its energy compared to the final electron energies, E_s and E_e, we arrive at the following expression for the cross section:

$$\frac{d\sigma}{dE_s dE_e d\Omega_s d\Omega_e} = \sum_{N=-\infty}^{\infty} d^3\sigma_N \times \delta(E_s + E_e - E_0 - \mathcal{E}_{H_2^+} + U_p + N\omega), \qquad (9)$$

where $U_p = F_0^2/4\omega^2$ is the ponderomotive potential. Equation (9) has a form of a sum over processes with different number of emitted ($N > 0$) or absorbed ($N < 0$) photons [6]. The N-photon triple differential cross section (TDCS) is given by

$$\frac{d^3\sigma_N}{dE_s d\Omega_s d\Omega_e} = \frac{1}{(2\pi)^3} \frac{p_s p_e}{p_0} \left(\frac{d\sigma}{d\Omega} \right)_{ee} \times \langle \psi_g | \mathcal{F}_N(\boldsymbol{R}, \boldsymbol{q}) \mathcal{F}_N^*(\boldsymbol{R}, \boldsymbol{q}) | \psi_g \rangle, \qquad (10)$$

where $(d\sigma/d\Omega)_{ee}$ is the half-off-shell Mott-scattering cross section that takes account of exchange between the colliding electrons, and

$$\mathcal{F}_N(\boldsymbol{R}, \boldsymbol{q}) = \frac{\omega}{2\pi} \int_{-\pi/\omega}^{\pi/\omega} dt e^{-i\left(N\omega + U_p + \frac{q^2}{2}\right)t} \times \left[\langle \chi_{\boldsymbol{q}} | \phi_g \rangle - \frac{\langle \phi_g | \boldsymbol{r} \boldsymbol{F}(t) | \phi_u \rangle}{E_u - E_g} \langle \chi_{\boldsymbol{q}} | \phi_u \rangle \right] \qquad (11)$$

is the laser-assisted momentum profile.

3 Results and discussion

In this section we present the results of numerical calculations of the laser-assisted TDCS in symmetric noncoplanar EMS kinematics (see Fig. 1 and Ref. [19,20]). In this kinematics, the scattered and ejected electron angles

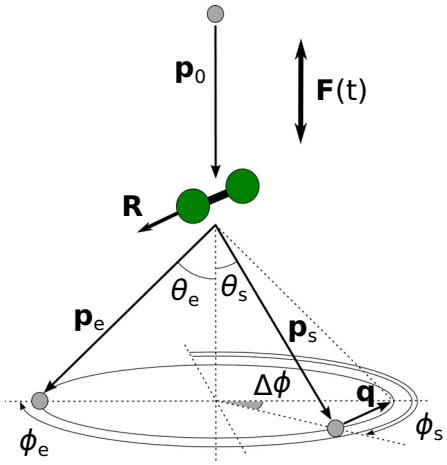

Fig. 1. Schematic representation of symmetric noncoplanar EMS kinematics.

with respect to the incident electron direction are $\theta_s = \theta_e = 45°$, and the scattered and ejected electron energies are $E_s = E_e = E$. The TDCS is studied as a function of q, which is varied by scanning the out-of-plane azimuthal angle of the scattered electron ϕ_s. We consider such value of the incident electron energy, namely $E_0 = 6$ keV $- \mathcal{E}_{H_2^+}$, and such range of q values that in the absence of the laser field the effects of distortion of the plane waves and the second Born effects are expected to be subsidiary (see Ref. [20] for details). The laser field orientation is chosen such that its electric component $\boldsymbol{F}_0$ is parallel to $\boldsymbol{p}_0$. Bearing in mind a possible experimental realization [4], the laser frequency and intensity are set to $\omega = 1.55$ eV and $I = 5 \times 10^{11}$ W/cm^2, respectively.

We consider the TDCS for an unoriented molecular ion, averaging over the initial rotational and vibrational states. Figure 2 shows how the field-free TDCS is modified by the presence of a laser field. For comparison, TDCS results for an unperturbed model of the initial ionic state are also shown. In that case the laser field does not affect the initial target state, so that (cf. Eq. (8))

$$\Psi_i = \psi_g(\boldsymbol{R}, t)\phi_g(\boldsymbol{r}, \boldsymbol{R}, t); \qquad (12)$$

however, its influence on the fast incoming and outgoing electrons is taken into account by describing them with Volkov functions.

When the total number of photons exchanged between the colliding system and the field is $N = 0$, the laser-field effect is diminishing, such that field-dressed and field-free momentum profiles cannot be distinguished. Figure 2 also shows numerical results for $N = \pm 1$ laser-assisted TDCS. While they exhibit a qualitatively similar behavior to the $N = 0$ case, they are much smaller in magnitude. This is explained by the low intensity of the laser field – the probability of multiphoton processes rapidly decreases when the number of involved photons increases. Since the electric-field amplitude is rather small on the atomic scale, $F_0 \approx 0.004$ a.u., one might expect the unperturbed and quasistatic models to give indistinguishable results. However, the corresponding cross sections display certain differences, which are due to the admixture of the antibonding orbital ϕ_u in the quasistatic state ϕ_1 that evolves from the unperturbed bonging orbital ϕ_g (see Eq. (6)).

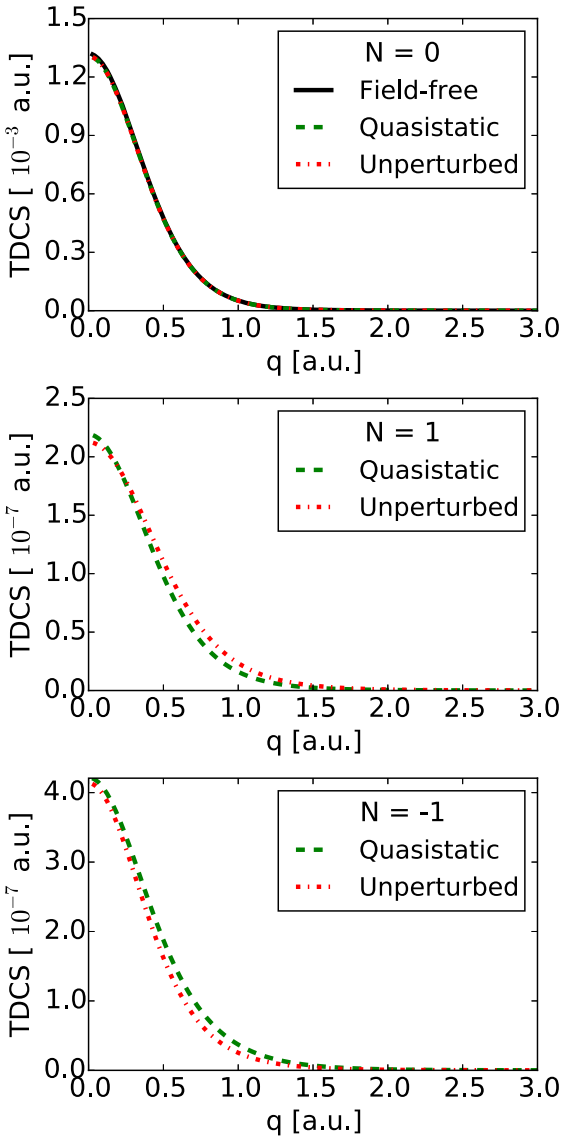

Fig. 2. Field-free and laser-assisted $N = 0, \pm 1$ TDCS for quasistatic (8) and unperturbed (12) initial state models of the H_2^+ ion.

Let us turn to the investigation of bond oscillation. In the field-free case its nature can be seen by switching to momentum representation of the target initial state [11]:

$$\phi_g(\boldsymbol{q}) = N_g \phi_{1s}(\boldsymbol{q})[\exp(i\boldsymbol{q}\boldsymbol{R}/2) + \exp(-i\boldsymbol{q}\boldsymbol{R}/2)]. \qquad (13)$$

Averaging its absolute square over the $\boldsymbol{R}$ direction, we get the momentum profile of the unoriented $1\sigma_g$ orbital as

$$|\mathcal{F}_{1\sigma_g}(\boldsymbol{q})|^2 = 2|N_g|^2|\phi_{1s}(\boldsymbol{q})|^2 \left(1 + \frac{\sin(qR)}{qR}\right), \qquad (14)$$

where $|\phi_{1s}(\boldsymbol{q})|^2$ is the momentum profile of the $1s$ atomic hydrogen orbital. The last factor, $[1+\sin(qR)/qR]$, induces

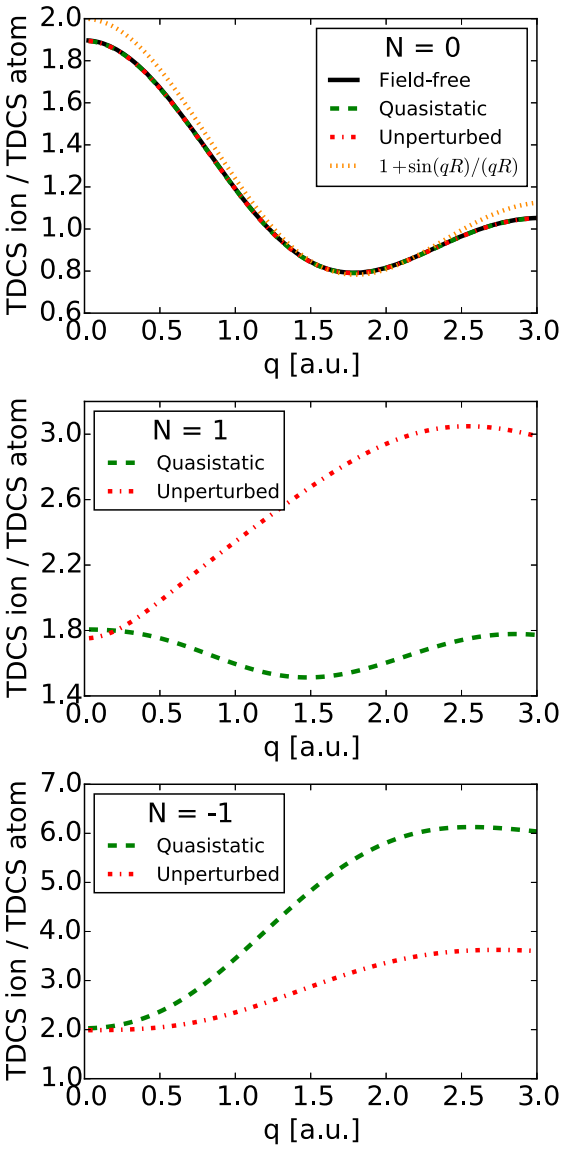

Fig. 3. Ratio of ionic to atomic TDCS demonstrating bond oscillation for field-free and laser-assisted $N = 0, \pm 1$ cases.

oscillations in the momentum profile depending on the internuclear distance and is responsible for bond oscillation effects. In the field-free case, it can be clearly observed by computing the ratio of the molecular and atomic TDCS. The latter is given by

$$\frac{d^3\sigma}{dE_s d\Omega_s d\Omega_e} = \frac{1}{(2\pi)^3}\frac{p_s p_e}{p_0}\left(\frac{d\sigma}{d\Omega}\right)_{ee} |\phi_{1s}(\boldsymbol{q})|^2. \quad (15)$$

The ratio is plotted as 'Field-free' in the top panel of Figure 3.

In the laser-assisted case, the bond oscillation factor is given by the ratio of the laser-assisted cross section for the hydrogen molecular ion to that for the atomic hydrogen. We calculate the laser-assisted atomic cross section using the unperturbed hydrogen wave function and describing the incoming and outgoing electrons with Volkov functions (see, for instance, Refs. [6,7] for details). The use of the unperturbed wave function in the atomic case is justified by the weak dressing of the hydrogen ground state in the considered laser field, in contrast to the molecular case, where the laser field effectively couples the states (4) and (5). The laser field has no appreciable effect in the $N = 0$ case, with the laser-assisted interference pattern being indistinguishable from the field-free one. Contrary to $N = 0$, in the $N = \pm 1$ case, quasistatic and unperturbed models yield markedly different results, signifying the importance of the field-dressing effects even at moderate intensities. The observed difference is explained by the contribution from the $1\sigma_u$ orbital to the quaistatic state. The field-free wave function of this orbital in momentum space is

$$\phi_u(\boldsymbol{q}) = N_u \phi_{1s}(\boldsymbol{q})[\exp(i\boldsymbol{qR}/2) - \exp(-i\boldsymbol{qR}/2)]. \quad (16)$$

Hence, the momentum profile of the unoriented $1\sigma_u$ orbital is given by

$$|\mathcal{F}_{1\sigma_u}(\boldsymbol{q})|^2 = 2|N_u|^2|\phi_{1s}(\boldsymbol{q})|^2\left(1 - \frac{\sin(qR)}{qR}\right). \quad (17)$$

Comparison of equations (14) and (17) shows that the bond-oscillation factors for the $1\sigma_g$ and $1\sigma_u$ orbitals are qualitatively different. At the same time, the momentum profile (17) is not accessible in the case of the field-free EMS, since the H_2^+ ion in the antibonding $1\sigma_u$ state is unstable. In the laser-assisted case, the effect of the $1\sigma_u$ component in the quasistatic state can be probed. From the presented numerical results it follows that the laser-assisted bond-oscillation factors exhibit much larger sensitivity to this effect than the laser-assisted momentum profiles.

4 Summary and conclusions

A theoretical analysis of laser-assisted electron-impact ionization of the hydrogen molecular ion H_2^+ in the EMS kinematical regime has been presented. We performed numerical calculations for $(e, 2e)$ TDCS on H_2^+ assisted by N-photon absorption or emission using a quasistatic states approach to accommodate the laser-field influence on the molecular ion. In the case of the laser-field parameters that can be realizable in experiment (see Refs. [4,5] for details), we found that the laser-assisted momentum profiles are weakly sensitive to the presence of laser radiation in the $N = 0$ case. However, when a single photon is emitted or absorbed during the collision process, cross sections obtained with quasistatic and unperturbed models of the target state can be distinguished. The differences are much more pronounced in the bond-oscillation effect, where notable sensitivity of an interference factor to the employed field-dressed target states is observed even for moderate strength of the laser field.

We are grateful to S.I. Vinitsky and O. Chuluunbaatar for useful discussions. The work of A.A.B. was supported by the Russian Foundation for Basic Research (Grant No. 16-32-00428 мол_а).

References

1. V.G. Neudatchin, Yu.V. Popov, Yu.F. Smirnov, Phys. Usp. **42**, 1017 (1999)
2. E. Weigold, I.E. McCarthy, *Electron Momentum Spectroscopy* (Kluwer Academic/Plenum Publishers, New York, 1999)
3. M. Takahashi, Bull. Chem. Soc. Jpn **82**, 751 (2009)
4. M. Yamazaki, Y. Kasai, K. Oishi, H. Nakazawa, M. Takahashi, Rev. Sci. Instum. **84**, 063105 (2013)
5. M. Yamazaki, K. Oishi, H. Nakazawa, C. Zhu, M. Takahashi, Phys. Rev. Lett. **114**, 103005 (2015)
6. K.A. Kouzakov, Yu.V. Popov, M. Takahashi, Phys. Rev. A **82**, 023410 (2010)
7. A.A. Bulychev, K.A. Kouzakov, Yu.V. Popov, Phys. Lett. A **376**, 484 (2012)
8. A.A. Bulychev, K.A. Kouzakov, Eur. Phys. J. D **68**, 354 (2014)
9. A.A. Bulychev, K.A. Kouzakov, Phys. Rev. A **91**, 023413 (2015)
10. N. Watanabe, X.-J. Chen, M. Takahashi, Phys. Rev. Lett. **108**, 173201 (2012)
11. M. Yamazaki, H. Satoh, N. Watanabe, D.B. Jones, M. Takahashi, Phys. Rev. A **90**, 052711 (2014)
12. M. Zhao, Xu. Shan, J. Yang, E. Wang, S. Niu, X. Chen, Chin. J. Chem. Phys. **28**, 539 (2015)
13. D.M. Volkov, Z. Phys. **94**, 250 (1935)
14. M.V. Fedorov, *Atomic and free electrons in a strong light field* (World Scientific, Singapore, 1997)
15. A.A. Bulychev, K.A. Kouzakov, Yu.V. Popov, Proc. of SPIE **8699**, 86991B (2013)
16. I. Kawata, H. Kono, Y. Fujima, J. Chem. Phys. **110**, 11152 (1999)
17. F. Kelkensberg, G. Sansone, M. Ivanov, M. Vrakking, Phys. Chem. Chem. Phys. **13**, 8647 (2011)
18. V.S. Yakovlev, M. Korbman, A. Scrinzi, Chem. Phys. **414**, 26 (2013)
19. N. Watanabe, Y. Khajuria, M. Takahashi, Y. Udagawa, P.S. Vinitsky, Yu.V. Popov, O. Chuluunbaatar, K.A. Kouzakov, Phys. Rev. A **72**, 032705 (2005)
20. N. Watanabe, Y. Udagawa, M. Takahashi, K.A. Kouzakov, Yu.V. Popov, Phys. Rev. A **75**, 052701 (2007)